

SODIUM-RICH ANTIPEROVSKITE STUDIES

Modern studies relating to conductivity

LEGEND:



EXP.



DFT DEF.



PB DEF.



DFT NEB

















































PB NEB








































DFT AIMD

















PB MD

PAPER	FOCUS	MATERIALS	SYNTHESIS/MODEL	CONCLUSIONS
<i>Structural manipulation approaches towards enhanced sodium ionic conductivity in Na-rich antiperovskites</i> WANG, 2015	Developing a facile and timesaving synthetic route; improving conductivity of antiperovskite via alio- and isovalent doping	 $\text{Na}_3\text{OCl}_{1-x}\text{Br}_x$ ($x = 0 - 1$)  $\text{Na}_3\text{OBr}_{1-x}\text{I}_x$ ($x = 0 - 1$)  $\text{Na}_{2.9}\text{M}_{0.05}\text{OBr}_{0.6}\text{I}_{0.4}$ ($\text{M} = \text{Ca}, \text{Sr}$)  Na_3OX ($\text{X} = \text{Cl}, \text{Br}, \text{I}$)	Solid-state reaction + heating @ 350 °C for 3h CASTEP for NEB	Facile, timesaving route successful; alio- and isovalent doping is a promising mean of increasing conductivity: NSOBI in the mS/cm range @ 200 °C
<i>Sodium ion transport mechanisms in antiperovskite electrolytes Na_3OBr and Na_4OI_2: an in situ neutron diffraction study</i> ZHU, 2016	Understanding the sodium transport pathway in bulk and layered antiperovskites, via neutron diffraction and maximum entropy method	 Na_3OBr  Na_4OI_2  Na_3OBr  Na_4OI_2	Solid-state reaction + heating @ 400 °C for 4h CASTEP for NEB	Main sodium transport pathway between nearest sodium ions in Na_6O octahedra (both cubic and layered); in layered I^- ions act as bridges between octahedra
<i>Experimental and computational evaluation of a sodium-rich antiperovskite for solid state electrolytes</i> NGUYEN, 2016	Increase ionic conductivity in antiperovskites via a post-processing method, spark plasma sintering (SPS)	 Na_3OBr  Na_3OBr	Solid-state reaction + heating @ 450 °C for 24h, then SPS VASP for DEFECTS	SPS reduces interfacial impedance and activation energy, but conductivity in 10^{-7} S/cm range, due to lack of defects
<i>A first principle study of the phase stability, ion transport and substitution strategy for highly ionic conductive sodium antiperovskite as solid state electrolytes for sodium ion batteries</i> WAN, 2018	Improving understanding of defects in antiperovskites an improving conductivity in these materials via aliovalent doping with alkaline earth ions	 Na_3OCl  Na_3OCl  $\text{Na}_3\text{M}_{1/\infty}\text{OCl}$ ($\text{M} = \text{Mg}, \text{Ca}, \text{Sr}, \text{Ba}$)  $\text{Na}_{2.875}\text{OCl}$  $\text{Na}_{2.75}\text{Ca}_{0.125}\text{OCl}$	VASP for DEFECTS, NEB and AIMD	NaCl Schottky is most favourable; alkaline earth doping increases activation energy of vacancy hops, but also increases defect concentration, so overall it can affect conductivity positively
<i>Theoretical design of a double-antiperovskite Na_6SOI_2 as a super-fast ion conductor for solid Na^+ ion batteries</i> YU, 2018	Exploration of a sodium double antiperovskite as a solid state electrolyte, observing stability, conductivity and and compatibility with electrodes	 Na_6SOI_2  $\text{Na}_{25}\text{S}_5\text{O}_4\text{I}_7$  $\text{Na}_{23}\text{S}_4\text{O}_4\text{I}_8$  $\text{Na}_{25}\text{O}_9\text{Cl}_7$  $\text{Na}_{23}\text{O}_8\text{Cl}_8$	VASP for DEFECTS and AIMD	Off-stoichiometric double-antiperovskites are predicted with low activation barriers and ultra-fast conductivity around 10 ms/cm; stability was also good
<i>Composititon screening of lithium- and sodium-rich anti-perovskites for fast-conducting solid electrolytes</i> DAWSON, 2018	Investigation of defect formation energies and sodium ion transport capabilities in Li/Na antiperovskites with alkali-mixing and isovalent doping of the halides	 $\text{Na}_{3-x}\text{Li}_x\text{OX}$ ($x = 1, 2; \text{X} = \text{Cl}, \text{Br}$)  $\text{Na}_3\text{OCl}_{1-x}\text{Br}_x$ ($x = 0, 0.5, 1$)  $\text{Na}_{3-x}\text{Li}_x\text{OX}$ ($x = 1, 2; \text{X} = \text{Cl}, \text{Br}$)  $\text{Na}_3\text{OCl}_{1-x}\text{Br}_x$ ($x = 0, 0.5, 1$)  $\text{Na}_{3-x}\text{Li}_x\text{OX}$ ($x = 1, 2; \text{X} = \text{Cl}, \text{Br}$)  $\text{Na}_3\text{OCl}_{1-x}\text{Br}_x$ ($x = 0, 0.5, 1$)	GULP for DEFECTS and NEB LAMMPS for MD	Schottky MCl defect are favourable; mixed Li\Na systems do not provide enhanced conductivity; mixing halides could be used to finetune activation energies; max conductivity was still only around 5 mS/cm at 500K
<i>Sodium superionic conductors based on clusters</i> FANG, 2019	Improving conductivity via cluster anions, that i, have good tolerance factor ii, create large channels iii, soften the lattice	 $\text{Na}_3\text{S}(\text{BCl}_4)$  $\text{Na}_{2.875}\text{OX}$ ($\text{X} = \text{Br}, \text{BF}_4, \text{AlH}_4$)  $\text{Na}_{2.875}\text{S}(\text{BCl}_4)$  $\text{Na}_{2.875}\text{S}(\text{BCl}_4)_{0.5}\text{I}_{0.5}$	VASP for NEB and AIMD	Substitution of cluster anions is effective in creating larger channels and softer lattices that lead to conductivities of mS/cm at RT for $\text{Na}_3\text{S}(\text{BCl}_4)$ and $\text{Na}_3\text{S}(\text{BCl}_4)_{0.5}\text{I}_{0.5}$
<i>Rotational cluster anion enabling superionic conductivity in sodium-rich antiperovskite Na_3OBH_4</i> SUN, 2019	Attempting synthesis of antiperovskites with best tolerance factor from Na_3XY ($\text{X} = \text{O}, \text{S}; \text{Y} = \text{BH}_4, \text{BF}_4$)	 Na_3OBH_4	Solid-state reaction?	The rotation of the tetrahydroborate failitates ion movement hence increasing conductivity significantly
<i>Theoretical tuning of Ruddlesden-Popper type anti-perovskite phases as superb ion conductors and cathodes for solid sodium ion batteries</i> YU, 2019	Investigation of a range of sodium-rich Ruddlesden-Popper antiperovskites for solid state electrolyte applications, in terms of conductivity and stability	 $\text{Na}_4\text{O}_{1-x}\text{S}_x\text{Cl}_{1-y}\text{I}_y$ ($x = 0, 1; y = 0, 1, 2$)  Na_4OI_2  Na_4OICl  $\text{Na}_4\text{S}_{0.5}\text{O}_{0.5}\text{I}_2$  $\text{Na}_3\text{LiS}_{0.5}\text{O}_{0.5}\text{I}_2$	VASP for DEFECTS and AIMD	'Superb' electrolyte $\text{Na}_3\text{LiS}_{0.5}\text{O}_{0.5}\text{I}_2$ with RT conductivity of 6.3 mS/cm; electrolyte is predicted to be compatible with sodium anode both electrochemically and thermodynamically
<i>Correlating lattice distortions, ion migration barriers, and stability in solid electrolytes</i> KIM, 2019	Probing the connection between ionic mobility, thermodynamic stability and symmetry-lowering distortions	 Na_3OX ($\text{X} = \text{F}, \text{Cl}, \text{Br}, \text{I}$)  Na_3SX ($\text{X} = \text{F}, \text{Cl}, \text{Br}, \text{I}$)  Na_3SeX ($\text{X} = \text{F}, \text{Cl}, \text{Br}, \text{I}$)	VASP for NEB	Increasing the degree of distortion (deviating tolerance factor for ideal) leads to lower migration energy, but also lower stability; Na_3SI could be the balance
<i>Mechanochemical synthesis and ion transport properties of Na_3OX ($\text{X} = \text{Cl}, \text{Br}, \text{I}$ and BH_4) andtiperovskite solid electrolytes</i> AHIIVI, 2020	Investigation of synthesis and experimental conductivity of various sodium antiperovskites; test of ball-milling method	 Na_3OX ($\text{X} = \text{Cl}, \text{Br}, \text{BH}_4$)  $\text{Na}_3\text{OX}_{0.5}(\text{BH}_4)_{0.5}$ ($\text{X} = \text{Cl}, \text{Br}$)  $\text{Na}_3\text{OCl}_{0.33}\text{Br}_{0.33}(\text{BH}_4)_{0.33}$  Na_3OX ($\text{X} = \text{Cl}, \text{Br}, \text{I}, \text{BH}_4$)	Soli-state reaction with ball-milling + heating @ 200 °C for 13h VASP for AIMD	Ball-milling works well as cheap and effective synthesis; larger (super)halogens lead to lower activation energy with both channel size and polarizability
<i>Mechanism of enhanced ionic conductivity by rotational nitrite group in antiperovskite Na_3ONO_2</i> GAO, 2020	Attempt at synthesissing and measuring the conductivity of cluster antiperovskite Na_3ONO_2	 Na_3ONO_2	Solid-state reaction + heating @ 210 °C for 12h	Rotation of the anion unlocked above 200 °C, at which point activation is 0.385eV and conductivity of 0.37 mS/cm
<i>Theoretical study of Na^+ transport in the solid-state electrolyte Na_3OBr based on deep potential molecular dynamics</i> LI, 2020	Exploration of the DeePMD approach for antiperovskites	 Na_3OBr  Na_3OBr	DeePMD for NEB and MD	DeePMD produces data with good consitstency with previous experiments, while provodong a cheaper alternative to ab initi methods

<i>A Na-rich fluorinated sulfate anti-perovskite with dual doping as solid electrolyte for Na metal solid state batteries</i> FAN, 2020	Synthesising and investigating the structure and conductivity of a novel sulfate-based antiperovskite	 $\text{Na}_3\text{SO}_4\text{F}$ $\text{Na}_{2.98}\text{Mg}_{0.01}\text{SO}_4\text{F}_{0.95}\text{Cl}_{0.05}$	Ball-milling with alcohol + heating @ 500 °C for 36h	Material is promising with conductivities in the 0.01 mS/cm range when doped with alkaline earth and large halide ions
<i>Facile synthesis and electrochemical properties of Na-rich anti-perovskite solid electrolytes</i> FENG, 2020	A low-temperature synthesis method for antiperovskites	 $\text{Na}_3\text{OBr}_{1-x}\text{I}_x$ (x = 0, 0.3, 0.5, 0.7, 1)	Solid-state reaction with ball-milling + heating @ 250 °C for 12h	Sharp drop in conductivity as temperature is lowered, possibly from change of structural symmetry and Na sites
<i>Superionic conduction in low-dimensional-networked anti-perovskites</i> LU, 2020	Investigating the effect of dimensionality on alkali ion connectivity in antiperovskites	 Na_3OX (X = Br, I) Na_4OX_2 (X = Br, I)	VASP for AIMD	Reducing the dimensionality of the octahedral networks effectively lowers the Li diffusion barrier, due to the enlarged
<i>Hydride-based antiperovskites with soft anionic sublattices as fast alkali ionic conductors</i> GAO, 2021	Soft anions for stability of cubic structure and softening of phonon mode of octahedral rotation	 Na_3HCh (Ch = S, Se, Te) $\text{Na}_{2.9}\text{HSe}_{0.9}\text{I}_{0.1}$  Na_3HCh (Ch = S, Se, Te)  Na_3HCh (Ch = S, Se, Te)	Solid-state reaction with SPS-like processing VASP for DEF. (natural) and NEB	NEB calculations showed low activations; after doping conductivity of $\text{Na}_{2.9}\text{HSe}_{0.9}\text{I}_{0.1}$ showed conductivities in the 10^{-4} S/cm at 100 °C

SODIUM-RICH ANTIPEROVSKITE STUDIES Early studies and modern studies relating to structural properties			LEGEND:  EXP.  DFT	
PAPER	FOCUS	MATERIALS	SYNTHESIS/MODEL	OUTCOMES
<i>New investigations of Na₃NO₃</i> JANSEN, 1977 	Discovering the structural properties of Na ₃ ONO ₂	 Na ₃ ONO ₂	?	Cubic antiperovskite with a = 4.605 Å
<i>The crystal-structure of kogarkoite, Na₃SO₄F</i> FANFANI, 1980 	Discovering the structural properties of Na ₃ SO ₄ F	 Na ₃ SO ₄ F	?	Monoclinic antiperovskite with a = 18.074, b = 6.958, c = 11.443 Å
<i>Na₃OCl and Na₃OBr, the 1st alkali-metal chalcogenide halides</i> SABROWSKY, 1988 	Discovering the structural properties of Na ₃ OCl and Na ₃ OBr	 Na ₃ OX (X = Cl, Br)	Sintering between 793 and 892 K	Both structures were cubic antiperovskite, with a = 4.500 and 4.573 Å, for the Cl and Br variant
<i>Na₄OI₂ - A new type of alkali-metal chalcogenide halide</i> SABROWSKY, 1989 	Discovering the structural properties of Na ₄ OI ₂	 Na ₄ OI ₂	Sintering between 773 and 823 K	Tetragonal antiperovskite with a = 4.677 and c = 26.020 Å
<i>Structure of Na₃OCl</i> HIPPLER, 1990 	Discovering the structural properties of Na ₃ OCl	 Na ₃ OCl	Sintering between 573 K and 873 K	Cubic antiperovskite with a = 4.496 Å
<i>Crystal-structure of Na₄OBr₂</i> HIPPLER, 1990 	Discovering the structural properties of Na ₄ OBr ₂	 Na ₄ OBr ₂	Sintering between 723 K and 773 K	Tetragonal antiperovskite with a = 4.521, c = 14.908 Å
<i>Structure of Na₄OI₂</i> SABROWSKY, 1990 	Discovering the structural properties of Na ₄ OI ₂	 Na ₄ OI ₂	Sintering at 830 K	Tetragonal antiperovskite with a = 4.655 and c = 15.940 Å
<i>Na₃O(CN) - The 1st alkali-metal chalcogenide pseudohalide</i> HIPPLER, 1990 	Discovering the structural properties of Na ₃ O(CN)	 Na ₃ O(CN)	Sintering between 640 K and 770 K	Cubic antiperovskite with a = 4.56 Å
<i>(CN)ONa₃, crystal structure and sodium ion conductivity</i> MULLER, 1990 	Measuring the structural properties sodium conductivity of Na ₃ O(CN)	 Na ₃ O(CN)	?	Above 230°C exceptionally high sodium ion conductivity (10 ⁻² S/cm) from the rotational disorder of the CN ⁻
<i>On the quasi-binary systems NaNO₂/Na₂O and NaCN/Na₂O, phase diagrams and sodium ion conductivity of Na₃O(NO₂) and Na₃O(CN)</i> JANSEN, 1992 	Improving understanding on the temperature-depend phase-transitions and their effect on conductivity in Na ₃ ONO ₂ and Na ₃ OCN	 Na ₃ ONO ₂  Na ₃ O(CN)	?	Sharp increase in conductivity at 200-250 °C as a consequence of a “melting” of the sodium sublattice or the rotational disorder of complex anions
<i>Lattice dynamics of antiperovskite structure compounds A₃OX (A = Na, K; X = Cl, Br)</i> ZIENKO, 2001 	Exploring the lattice dynamics of antiperovskite structures	 Na ₃ OX (X = Cl, Br)	DFT	Elastic moduli constants and dielectric constants
<i>Ab initio study of electronic structure, elastic and optical peoperties of anti-perovskite type alkali metal halides</i> RAMANNA, 2013 	Exploring elastic and optical properties for antiperovskite structures via both GGA and LDA methods	 Na ₃ OX (X = Cl, Br)	CASTEP for DFT	Elastic properties including bulk moduli, shear moduli, Young's moduli, Poisson's ratio, anisotropy factor and Cauchy's pressure
<i>Order-disorder phase transition in the antiperovskite-type structure of synthetic kogarkoite, Na₃SO₄F</i> AVDONTCEVA, 2015 	Improving understanding on the temperature-induced structural transformations in kogarkoite	 Na ₃ SO ₄ F	Evaporation from aqueous solution at 25 °C	Transofrmation involves complete disordering of the sulfate tetrahedra, antiperovskite octahedral framework intact
<i>Elastic properties of alkali superionic conductor electrolytes from first principles calculations</i> DENG, 2016 	Exploring elastic and optical properties for antiperovskite structures	 Na ₃ OX (X = Cl, Br)	VASP for DFT	Elastic properties including bulk moduli, shear moduli, Young's moduli, Poisson's ratios and Pough's ratios

<p><i>Robust high pressure stability and negative thermal expansion in sodium-rich antiperovskites</i> Na_3OBr and Na_4OI_2</p> <p>WANG, 2016</p>  	<p>Investigation of structural variability of antiperovskites under high pressures and low temperatures</p>	 Na_3OBr Na_4OI_2  Na_3OBr Na_4OI_2	<p>Solid-state reaction + heating @ 350 °C for 3h</p> <p>CASTEP for DFT</p>	<p>Both structures stable up to 23 GPa; negative thermal expansion at very low temperatures; phase stability, symmetry preferences explained qualitatively</p>
<p><i>Electronic, elastic, lattice dynamic and thermal conductivity properties of Na_3OBr</i></p> <p>LV, 2017</p> 	<p>Investigation of various structural properties for the antiperovskite Na_3OBr</p>	 Na_3OBr	<p>CASTEP for DFT</p>	<p>Properties include bulk, shear, and Young's moduli, Poisson's and Pough's ratios; static + hf dielectric constant; thermal conductivity</p>
<p><i>Computational predictions of stable phase for antiperovskite Na_3OCl</i></p> <p>PHAM, 2018</p> 	<p>Investigation of stability of non-cubic phases in antiperovskites, with potentially lower activations</p>	 Na_3OCl	<p>VASP for DFT</p>	<p>14 tilted structures energetically more stable than cubic $\text{Pm}\bar{3}\text{m}$, with $\text{P2}_1/\text{m}$ being most stable; the two phases have similar band gaps</p>
<p><i>Electronic structure, thermomechanical and phonon properties of inverse perovskite oxide (Na_3OCl): An ab initio study</i></p> <p>KHANDY, 2020</p> 	<p>Investigation of various structural properties for the antiperovskite Na_3OCl</p>	 Na_3OCl	<p>Wien2K for DFT</p>	<p>Properties include bulk, shear, and Young's moduli, Poisson's and Pough's ratios, anisotropy factor; thermal conductivity</p>
<p><i>The structural stability, lattice dynamics, electronic, thermophysical, and mechanical properties of inverse perovskites A_3OX: A comparative first-principles study</i></p> <p>SATTAR, 2020</p> 	<p>Investigation of various structural properties for the antiperovskites Na_3OX (X = Cl, Br, I)</p>	 Na_3OX (X = Cl, Br, I)	<p>Wien2K for DFT</p>	<p>Properties include bulk, shear, and Young's moduli, Poisson's and Pough's ratios, anisotropy factor; thermal conductivity</p>
<p><i>Synthesis of Antiperovskite Solid Electrolytes: Comparing Li_3SI, Na_3SI, and Ag_3SI</i></p> <p>YIN, 2020</p> 	<p>Attempt at synthesising iodide-based antiperovskites for larger channel size and faster conductivity</p>	 Na_3OI	<p>Solid-state reaction + heating @ up to 600 °C (with a 3 stage profile)</p>	<p>In the case of Na_3SI (and Li_3SI), the adoption of bcc anion packing in the reactants does not occur below melting point, which makes formation difficult</p>